A discrete population balance equation for binary breakage

Liao, Y.; Oertel, R.; Kriebitzsch, S.; Schlegel, F.; Lucas, D.;

Originally published:

February 2018

International Journal for Numerical Methods in Fluids 87(2018)4, 202-215

DOI: https://doi.org/10.1002/fld.4491

Perma-Link to Publication Repository of HZDR:

https://www.hzdr.de/publications/Publ-25920

A Discrete Population Balance Equation for Binary Breakage

Y. Lao[a,*], R. Oertel[a], S. Kriebitzsch[b], F. Schlegel[a], D. Lucas[a]

[a] *Helmholtz-Zentrum Dresden - Rossendorf, Institute of Fluid Dynamics, Bautzner Landstrasse 400, 01328 Dresden, Germany*
[b] *TU Bergakademie Freiberg, Institute of Energy Process Engineering and Chemical Engineering, Fuchsmühlenweg 9, 09599 Freiberg, Germany*

Abstract

The numerical solution of the population balance equation is frequently achieved by means of discretization, i.e., by the method of classes. An important concern of discrete formulations is the preservation of a chosen set of moments of the distribution, e.g. numbers and mass, while remaining flexible on the grid applied. As for the physical modeling of the breakup rate, two approaches exist. One type states the breakup rate of a mother particle and requires a function that describes the distribution of daughter particles. The other type gives the breakup rate between a mother and a daughter particle directly, usually under the assumption of binary breakage. The lack of an explicitly stated daughter size distribution function has implications on the formulation of the discrete equations, because existing formulations contain integrals over the daughter size distribution function. To the knowledge of the authors, no efficient formulations for this type of models exist. In the present work, a discrete formulation of the breakup terms due to binary breakage is proposed, which allows a direct implementation of both kinds of models and an efficient solution of the population balance equation, making it favorable for the coupling to computational fluid dynamics codes.

Keywords: Binary Breakup, Computational Fluid Dynamics, Incorporated Daughter Size Distribution, Method of Classes, Population Balance Equation

1. Introduction

The concept of population balance was first introduced by Hulburt & Katz (1964) and Randolph (1964) for the description of the dynamic behavior of particulate systems. Over the past five decades, population balance modeling found ever-increasing application in the field of chemical and pharmaceutical engineering. An extensive review was recently published by Ramkrishna & Singh (2014).

Meanwhile, integrating the solution of the population balance equation (PBE) into computational fluid dynamics (CFD) software is becoming a popular and promising way of taking into account polydispersity without spatially resolving all elements of the dispersed phase and their interactions. Thereby, local size changes may be considered, which affect the interfacial area density as well as the flow structure. Among other reasons, this information is required to predict heat- and mass transfer rates or the transition from the homogeneous to the heterogeneous regime in bubble columns. Numerous examples of such coupled methods can be found in the literature. For example, Cheung et al. (2013) and Liao et al. (2015) predicted the bubble size distribution

*Corresponding author
Email address: y.liao@hzdr.de (Y. Lao)

in pipe flows. Chen et al. (2005) and Bannari et al. (2008) simulated gas-liquid bubble columns. Li et al. (2013) and Sen et al. (2014) did numerical investigations on a fluidized-bed spray granulation process. Bellot et al. (2014) dealt with the complex behavior in gas-stirred ladles. Metzger (2016) studied the fast precipitation crystallization process.

A well accepted formulation of the PBE including aggregation and breakup as well as nucleation and growth is presented in Ramkrishna (1985, 2000) and Jakobsen (2008). Since the focus of this work lies on the breakup terms, we state the volume-based PBE as

$$\frac{\partial n(v)}{\partial t} = \underbrace{\int_v^\infty n(v')\Omega_t(v')\beta(v,v')\mathrm{d}v'}_{B(v)} - \underbrace{n(v)\Omega_t(v)}_{D(v)} , \tag{1}$$

where $n(v)$ represents the number density of particles with volume v. The source and sink terms $B(v)$ and $D(v)$ on the right hand side represent the birth rate of particles with volume v due to breakup of larger particles with volume v' and their death rate due to breakup into smaller particles, respectively. The function $\Omega_t(v')$ involved in the sources terms is typically referred to as a breakup kernel. It describes the total breakup rate of a mother particle of volume v'. The so-called daughter size distribution function $\beta(v,v')$ represents the probability that a daughter particle with volume v is generated by breakage of a mother particle with volume v'. Normal and beta distribution functions are often adopted for this purpose (Coulaloglou & Tavlarides, 1977; Lee et al., 1987; Martinez-Bazan et al., 1999; Laakkonen et al., 2006). Since no mass can be created or destroyed during the breakup of a particle, it must satisfy

$$\int_0^{v'} v\beta(v,v')\mathrm{d}v = v' . \tag{2}$$

Additionally, the following constraints must be fulfilled for binary breakage

$$\int_0^{v'} \beta(v,v')\mathrm{d}v = 2 , \tag{3a}$$

$$\beta(v,v') = \beta(v'-v,v') . \tag{3b}$$

These constraints express that only two daughter particles are generated per breakage event and that the β function is mirror-symmetrical with respect to $v = 0.5v'$. On the basis of Eq. 2 and Eq. 3a, the global conservation of particle numbers and mass is satisfied during binary breakage processes

$$\int_0^\infty B(v)\mathrm{d}v \Big/ \int_0^\infty D(v)\mathrm{d}v = 2 , \tag{4a}$$

$$\int_0^\infty vB(v)\mathrm{d}v \Big/ \int_0^\infty vD(v)\mathrm{d}v = 1 . \tag{4b}$$

Analytical solutions of the PBE are limited to very few and simple forms of kernels (McCoy & Madras, 2003; Singh, 2014; Pinar, 2015). A detailed discussion about numerical approaches is given by Bayraktar (2014). Stochastic methods (Meimaroglou & Kiparissides, 2007; Goodson & Kraft, 2004; Kruis et al., 2012)

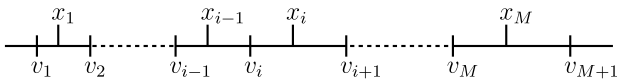

Figure 1: Discretization over the internal coordinate with representative sizes x_i and size group boundaries v_i

like Monte-Carlo simulations are comparatively slow but very exact. They are often used for the purpose of validating other methods. The method of moments (Wick et al., 2017; Madadi-Kandjani & A., 2015) is efficient, especially its quadrature-based version. Based on the rational that only averaged information about a distribution is relevant, a few low order moments need to be tracked. For example, if the PBE is written as a transport equation for the diameter-based number density function, then the Sauter mean diameter d_{32} can be determined by dividing the third by the second moment of the distribution. Since this is a relevant parameter for interfacial mass, energy and momentum exchange models in Euler-Euler simulations, it would be enough to solve for the zeroth to third moments. It is also possible to reconstruct the number density function from the moments as done by Yuan et al. (2012). The method of classes, also called discrete or sectional methods (Batterham et al., 1981; Hounslow et al., 1988; Kumar & Ramkrishna, 1996b) is an attractive and widely used alternative to the aforementioned approaches. It finds itself in between regarding the computational cost. Furthermore, its inherent information about the number density function is an appealing feature. The particle size is a fundamental property of any particulate system and it influences a variety of other properties, e.g., the settling and deposition of inhaled particles in the respiratory tract (Thomas, 2013). The method of classes is a popular method for coupling the PBE solution to a CFD simulation and also the focus of the current work.

Here, the class method with fixed pivots proposed by Kumar & Ramkrishna (1996a) is used. The continuous PBE (Eq. 1) is integrated over a size range $[v_i, v_{i+1}]$, which gives the total number of particles (or number concentration per control volume) N_i in this interval or class

$$N_i = \int_{v_i}^{v_{i+1}} n(v)\mathrm{d}v \ . \tag{5}$$

The terms on the right-hand side of Eq. eq:PBE are closed by utilizing the mean value theorem on the breakup rate. The integrals are expressed as sums over sub-intervals as defined by the discretization. The population of particles is assumed to be concentrated at representative sizes x_i, giving a source-term coupled set of differential equations for the number of particles in each interval

$$\frac{\partial N_i}{\partial t} = \underbrace{\sum_{j=i}^{M} N_j \Omega_t(x_j) \int_{v_i}^{v_{i+1}} \beta(v, x_j)\mathrm{d}v}_{B(x_i)} - \underbrace{N_i \Omega_t(x_i)}_{D(x_i)} \ . \tag{6}$$

A possible discretization over the internal coordinate is sketched in Fig. 1. Each class is given by its two boundary values v_i and v_{i+1}, which may be positioned in the middle of two adjacent representative values, i.e., $v_i = (x_{i-1} + x_i)/2$. The interval width of class i is $\Delta v_i = v_{i+1} - v_i$. For more details the reader is referred to Kumar & Ramkrishna (1996a).

As shown in Fig. 2, the daughter particles generated by breakup may have sizes different from the representative values of the classes. For example, if a particle with the representative volume x_j breaks up into one

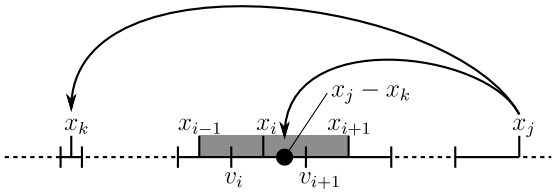

Figure 2: Breakup of a particle of volume x_j to a particle of volume x_k and its counterpart of volume $x_j - x_k$ falling into the interval $[x_i, x_{i+1}]$

daughter particle with the representative volume x_k, its counterpart with volume $v = x_j - x_k$ often falls between two classes, e.g. between classes i and $i+1$. If the resultant particles with a volume unequal to any pivot are assigned to the nearest class without adjustment, the mass and numbers would not be conserved in individual events (Bove, 2005). To guarantee mass and number conservation, i.e., internal consistency of the equations (Kumar & Ramkrishna, 1996a), both daughter particles have to be taken into account properly for each breakup event and the daughter size distribution function $\beta(v, x_j)$ in Eq. 6 should not simply be approximated by the mean value theorem, i.e., $\beta(v, x_j) = \beta(x_i, x_j)$. Therefore, the birth term requires further mathematical manipulation. The focus of the present work is a discrete formulation which works well for all breakup kernel types. The formulation is efficient for application in CFD and ensures both mass and number conservation. The paper is structured as follows: in Sect. 2 we discuss some limitations in existing formulations. An alternative discrete formulation is presented in Sect. 3 and its validation in Sect. 4. Finally, Sect. 5 concludes the paper.

2. Previous work

For the framework of breakup modeling, two different approaches are commonly used. Many breakup models such as those of Coulaloglou & Tavlarides (1977), Lee et al. (1987), Tsouris & Tavlarides (1994) and Martinez-Bazan et al. (1999) use the classical framework given in Eq. 1, i.e., they employ a total breakup rate $\Omega_t(v')$ and a separate continuous function for the daughter size distribution $\beta(v, v')$. Other breakup models such as Luo & Svendsen (1996), Lehr et al. (2002), Wang et al. (2003), Zhao & Ge (2007), Liao et al. (2011) and Xing et al. (2015) introduce kernels with an incorporated binary daughter size distribution, thereby providing the partial breakup rate $\Omega_p(v, v')$ directly. It is mirror-symmetrical about $v = v'/2$ and defined by the product of the total breakup rate and the daughter size distribution

$$\Omega_p(v, v') = \Omega_t(v')\beta(v, v') \; . \tag{7}$$

As discussed in Sect. 1 for β, an approximation of Ω_p using the mean value theorem will also lead to inconsistency. When a partial breakup model is used in combination with a discrete formulation that is based on a total breakup rate and a continuous daughter size distribution function, the total breakup rate needs to be calculated for each representative value

$$\Omega_t(v') = \frac{1}{2} \int_0^{v'} \Omega_p(v, v') \mathrm{d}v \; . \tag{8}$$

In a CFD simulation where the breakup rate depends on flow field parameters, the above integration would need to be carried out for each control volume (Wang & Wang, 2007; Bannari et al., 2008), thereby increasing the computational cost.

In the course of developing a discrete formulation that guarantees the conservation of mass and finally also numbers, many techniques were proposed, frequently with a pure focus on coalescence. Considering particles consisting exclusively of $x_i = 2^{i-1}$ monomers, Vanni (2000) extended the work of Batterham et al. (1981) for pure coalescence to the case of breakup. It was shown to be poor in capturing the shape of the number density function due to the very coarse grid. In addition, the formulation fails in preserving the total particle number, in spite of being mass conservative, as stated by Kumar & Ramkrishna (1996a).

An approximate method proposed by Marchal (1988) has no restriction on the choice of the representative values and boundaries. However, it has a restriction on the distribution of daughter particles. Their formulation is only applicable in cases where the size of the two daughters is precisely known (Vanni, 2000).

Hill et al. (1995) and Vanni (1999) tried to remove the inconsistency error by introducing correction factors in the birth and death terms. Hill et al. (1995) determined these factors by evaluating the budget of the zeroth and first moment, aiming at a correct prediction of numbers and total mass. The method was tested for a total breakup rate with a power law form against theoretical and empirical daughter particle size distributions. It was shown that in all cases mass is conserved, but the total number of particles is not correct in most cases.

The approximation method proposed by Vanni (1999) differs from that by Hill et al. (1995) only in the choice of the second constraint for the determination of the correction factors. Instead of a correct prediction of the total number of particles, they evaluated the net rate at which particles disappeared from each class from the uncorrected PBE. The corrected death term was set equal to this rate.

For pure coalescence Gelbard & Tambour (1980) derived a general conservation equation for the quantity q

$$q = \alpha v^{\gamma} n(v), \tag{9}$$

where α and γ are constants, by applying the mean value theorem on the number density $n(v)$ instead of the breakup rate. In this way, the preservation of the γ th moment is satisfied automatically, but not those of the moments with order different from γ. The approach was extended by Vanni (2000) to breakup events.

Keeping in mind, that the discrete formulation should exhibit number and mass conservation for any given discretization over the internal coordinate, a very general and established framework was proposed by Kumar & Ramkrishna (1996a). A benchmark study of several formulations for cases where coalescence and breakup occur simultaneously was conducted by Vanni (2000). He concluded that the method of Kumar & Ramkrishna (1996a) is favorable with respect to accuracy, efficiency and robustness. Therefore, it is used as a reference in the present work. If a particle breaks into particles with sizes other than the representative ones given by the discretization, this method allocates fractions between the two nearest neighbors. The fractions can be calculated in a way that guarantees the preservation of two chosen moments of the distribution, e.g. numbers and mass. For the latter, the discrete birth and death terms representing breakup are expressed as

$$B(x_i) = \sum_{j=i}^{M} \eta_{ji} N_j \Omega_t(x_j) \ ,$$

$$D(x_i) = N_i \Omega_t(x_i) \ .$$

The coefficient

$$\eta_{ji} = \int_{x_i}^{x_{i+1}} \frac{x_{i+1} - v}{x_{i+1} - x_i} \beta(v, x_j) \mathrm{d}v + \int_{x_i - 1}^{x_i} \frac{v - x_{i-1}}{x_i - x_{i-1}} \beta(v, x_j) \mathrm{d}v \tag{10}$$

The first and second term reduce to zero for $i = j$ and $i = 1$. Like all other methods discussed above it is based on the classical framework and efficient if analytical expressions for the daughter size distribution are available, or if its integration over v is manageable at low computational cost. If a partial breakup rate model is used, the framework cannot be directly and readily applied anymore. As discussed at the beginning of this section, Ω_t and β need to be obtained using Eq. 7 and 8, which affects the performance of a CFD simulation. Hagesaether et al. (2002) introduced a formulation for partial breakup kernels stating

$$\begin{aligned} B(x_i) = & \sum_{j=i+1, i\neq M}^{M} N_j \Omega_p'(x_i, x_j) \\ & + \sum_{j=1, i\neq M}^{i} \chi_{i+1,j} N_{i+1} \Omega_p'(x_j, x_{i+1}) \\ & + \sum_{j=1, i\neq 1}^{i-1} \left(1 - \chi_{i+1,j}\right) N_i \Omega_p'(x_j, x_i) \ , \\ D(x_i) = & \sum_{j=1}^{i-1} N_i \Omega_p'(x_j, x_i) \ , \end{aligned}$$

where $\chi_{i,j} = 2^{1+j-i}$. However, this formulation is restricted to $x_{i+1}/x_i = 2$.

In the next section an efficient discrete formulation for binary breakage is given. It avoids the numerical integration of Eq. 8 and allows a direct use of partial as well as total binary breakup rate models. Furthermore it is flexible in terms of discretization over the internal coordinate while preserving both mass and numbers by fulfilling the conditions given by the Eqs. 2, 3 and 4.

3. An alternative discrete formulation

As discussed in Sect. 1, a binary breakage event may lead to the formation of particles with volumes different from the representative values if the mother and one daughter particle are positioned at a representative value. In this case, the mean value theorem should not be applied on β or Ω_p for these secondary particles to avoid inconsistency. In the new discrete formulation, these particles are accounted for through their complementary partners (x_k in Fig. 2), which may coincide with a representative volume. For that purpose, before the discretization of Eq. 1 the birth by breakup term $B(v)$ is rewritten to

$$\begin{aligned} B(v) = & \int_{v}^{\infty} n(v') \Omega_t(v') \beta(v, v') \theta(v \leq v'/2) \mathrm{d}v' \\ & + \int_{v}^{\infty} n(v') \int_{0}^{v'} \Omega_t(v') \beta(v'', v') \delta(v'' - (v' - v)) \theta(v'' \leq v'/2) \mathrm{d}v'' \mathrm{d}v' \ . \end{aligned} \tag{11}$$

The formulation in Eq. 11 exploits the symmetry relation for β given in Eq. 3b, by classifying the daughter particles into two groups, i.e., one smaller than half of the respective mother particle size and the other one larger than it. This is achieved through the step function

$$\theta(x) = \begin{cases} 0 & \text{if } x \text{ is false} , \\ 1 & \text{if } x \text{ is true} . \end{cases}$$

The integration over all possible mother particles v' remains as given in Eq. 1. The first term represents the breakage of v' into v for all daughter particles that are smaller than $v'/2$. The second term introduces an additional inner integral over the range of complementary daughter particles v''. For a given mother particle size v', the secondary daughter particle with size $v' - v''$ may contribute to the change of $n(v)$, as determined by the delta function $\delta(v'' - (v' - v))$. v'' is also set to be smaller than $v'/2$ in order for the second term to be active. Inversely this means, that the secondary daughter particle $v' - v''$ has a size greater than $v'/2$. The advantage of the reformulation becomes clear by deriving the discrete version. For that purpose, Eq. 11 is integrated over a size range $[v_i, v_{i+1}]$, giving

$$\begin{aligned} \int_{v_i}^{v_{i+1}} B(v) = & \int_{v_i}^{v_{i+1}} \int_{v}^{\infty} n(v')\Omega_t(v')\beta(v, v')\theta(v \leq v'/2)\mathrm{d}v'\mathrm{d}v \\ + & \int_{v_i}^{v_{i+1}} \int_{v}^{\infty} n(v') \int_{0}^{v'} \Omega_t(v')\beta(v'', v')\delta(v'' - (v' - v))\theta(v'' \leq v'/2)\mathrm{d}v''\mathrm{d}v'\mathrm{d}v . \end{aligned}$$

The integrals are expressed as sums over sub-intervals. The total breakup rate, $\Omega_t(v')$ and the daughter size distribution functions, $\beta(v, v')$ and $\beta(v'', v')$, are now approximated by the mean value theorem. Furthermore, the integral over the number density $n(v)$ is substituted by N_i using Eq. 5, yielding

$$\begin{aligned} B(x_i) = & \sum_{j=i}^{M} N_j\Omega_t(x_j)\beta(x_i, x_j) \int_{v_i}^{v_{i+1}} \theta(v \leq x_j/2)\mathrm{d}v \\ + & \sum_{j=i}^{M} \sum_{k=1}^{j} N_j\Omega_t(x_j)\beta(x_k, x_j) \int_{v_i}^{v_{i+1}} \delta(x_k - (x_j - v))\mathrm{d}v \int_{v_k}^{v_{k+1}} \theta(v'' \leq x_j/2)\mathrm{d}v'' . \end{aligned} \tag{12}$$

A further elimination of the remaining integrals gives

$$B(x_i) = \sum_{j=i}^{M} N_j \Big[\Omega_t(x_j)\beta(x_i, x_j)\Delta v_i(j) + \sum_{k=1}^{j} \Omega_t(x_j)\beta(x_k, x_j)Y_{ijk}\Delta v_k(j) \Big] . \tag{13}$$

Possible inconsistencies introduced by the mean value theorem may be compensated by an appropriate discretization of the Dirac function (Engquist et al., 2005). The discrete δ function for class i, referred to as regularized weight function Y_{ijk}, determines the fraction that is assigned to class i if a secondary daughter particle with size $x_j - x_k$ falls into the neighborhood of x_i. For the exact conservation of mass and numbers, it is given by

$$Y_{ijk} = \begin{cases} \dfrac{(x_j - x_k) - x_{i-1}}{x_i - x_{i-1}} & \text{if } x_{i-1} \leq x_j - x_k < x_i , \\ \dfrac{x_{i+1} - (x_j - x_k)}{x_{i+1} - x_i} & \text{if } x_i \leq x_j - x_k < x_{i+1} , \\ 0 & \text{else} . \end{cases} \tag{14}$$

Note that it is possible to achieve the preservation of any two chosen moments by adapting the function Y_{ijk}. For more details the reader is referred to Kumar & Ramkrishna (1996a).

The integrals over the step functions in Eq. 12 result in

$$\Delta v_i(j) = \begin{cases} v_{i+1} - v_i & \text{if } v_{i+1} \leq x_j/2 \ , \\ x_j/2 - v_i & \text{if } v_i < x_j/2 < v_{i+1} \ , \\ 0 & \text{if } v_i \geq x_j/2 \ . \end{cases}$$

The β function in Eq. 13 is now stated in discrete form. Combining with Eq. 7 and Eq. 8, the discrete form of the partial breakup rate states

$$\Omega_p(x_i, x_j) = \Omega_t(x_j)\beta(x_i, x_j) \ , \tag{15}$$

and that of the total breakup rate

$$\Omega_t(x_i) = \sum_{j=1}^{i} \Omega_p(x_j, x_i)\Delta v_i(j) \ . \tag{16}$$

As a result, the discrete formulation of the birth term in Eq. 13 is transformed into

$$\begin{aligned} B\left(x_i\right) = & \sum_{j=i}^{M} N_j \Big[\Omega_p(x_i, x_j)\Delta v_i(j) \\ & + \sum_{k=1}^{M} \Omega_p(x_k, x_j) Y_{ijk} \Delta v_k(j) \Big] \ , \end{aligned} \tag{17}$$

and the death by breakup term in Eq. 6, $D(x_i)$, is rewritten as

$$D\left(x_i\right) = N_i \sum_{j=1}^{i} \Omega_p(x_j, x_i)\Delta v_j(i) \ . \tag{18}$$

The formulation is therefore generally applicable for both frameworks of breakup modeling for the case of binary breakage. The implementation of models with an incorporated daughter size distribution is direct and efficient, since it avoids the integration in Eq. 8.

4. Numerical results

Following the case presented by Kumar & Ramkrishna (1996a), we assume pure breakage processes starting from a monodisperse initial condition

$$n(v, t_0) = \begin{cases} 0.05 & \text{if } v = 1\,\mathrm{m}^3 \ , \\ 0 & \text{otherwise} \ . \end{cases}$$

The numerical results are obtained for geometric grids, i.e., the class boundaries are calculated by $v_{i+1} = s v_i$ with $s > 1$. All results are compared with a reference solution obtained with the formulation of Kumar & Ramkrishna (1996a), denoted as "Reference" in subsequent figures. For each test case, the number density function

$$n(x_i, t) = \frac{N_i(t)}{v_{i+1} - v_i} \ ,$$

Case	Breakup rate	Daughter size distribution
1	$\Omega_t(v') = v'^2$	$\beta(v,v') = 2/v'$
2	$\Omega_t(v') = v'^2$	$\beta(v,v') = \frac{12}{v}\left(\frac{v}{v'}\right)\left(1-\frac{v}{v'}\right)$
3	$\Omega_t(v') = 0.4\frac{\epsilon^{1/3}}{(1+\alpha_g)v'^{2/9}}\exp\left[-0.08\frac{\sigma(1+\alpha_g)^2}{\rho_l\epsilon^{2/3}v'^{5/9}}\right]$	$\beta(v,v') = \frac{4.8}{v'}\exp\left[-4.5\left(\frac{2v-v'}{v'}\right)^2\right]$
4	$\Omega_p(v,v') = C_1\frac{1-\alpha_g}{v'}\left(\frac{\epsilon}{d'^2}\right)^{1/3}\int_{\xi_{\min}}^{1}\frac{(1+\xi)^2}{\xi^{11/3}}\exp\left[-\frac{12c_f\sigma}{C_2\rho_l\epsilon^{2/3}d'^{5/3}\xi^{11/3}}\right]\mathrm{d}\xi$ with $C_1 = 0.923$, $C_2 = 2.0$, $c_f = \left(\frac{v}{v'}\right)^{2/3} + \left(1-\frac{v}{v'}\right)^{2/3} - 1$, $\xi = \lambda/d'$, $\xi_{\min} = 11.4\eta$	

Table 1: Test cases for validation

the time development of the total particle number

$$M_0(t) = \sum_{i=1}^{M} x_i^0 N_i(t) \,,$$

and the Sauter mean diameter

$$d_{32}(t) = \frac{\sum_{i=1}^{M} d_i^3 N_i(t)}{\sum_{i=1}^{M} d_i^2 N_i(t)}$$

are presented.

The test cases, each applying a different breakup model, are summarized in Tab. 1. The first case, case 1, uses a power-law kernel in combination with a uniform daughter size distribution. An analytical solution is given by Ziff & McGrady (1985). The daughter size distribution for the second test case, case 2, assumes a beta distribution, as used by Lee et al. (1987). The third case, case 3, employs the model from Coulaloglou & Tavlarides (1977), which assumes an exponential function for the total breakup frequency and a normal function for the daughter size distribution. For case 1, 2 and 3, total breakup models with a separate daughter size distribution function are applied. These cases aim at a validation of the new formulation against an analytical solution and reference solutions based on the formulation of Kumar & Ramkrishna (1996a). It is expected that both formulations deliver a similar performance. In contrast to the first three cases, the last case, case 4, shows the benefits of the new formulation for partial breakup models with an incorporated daughter size distribution. The well-accepted model from Luo & Svendsen (1996) is applied for that purpose. As discussed in previous sections, the use of the new formulation in Eq. 13 has convincing advantages in this situation, since the model provides the partial breakup rate $\Omega_p(v_i, v_j)$ directly. On the other hand, if the reference formulation is applied, an additional numerical integration is required when solving Eq. 8 in order to obtain the daughter size distribution $\beta(v_i, v_j)$. This increases the computational cost. The parameters used for the test cases are $\alpha_g = 0.05$, $\rho_l = 997\,\mathrm{kg\,m^{-3}}$, $\rho_g = 1.0\,\mathrm{kg\,m^{-3}}$, $\sigma = 0.072\,\mathrm{N\,m^{-1}}$, $\epsilon = 0.001\,\mathrm{m^2\,s^{-3}}$, and $\mu_l = 0.0008899\,\mathrm{Pa\,s^{-1}}$.

Case 1. Figure 3a and 3b show a comparison between the numerical and the analytical particle number density $n(v)$. Note that for the class representing the smallest particle size, the lower boundary v_1 is set to the value

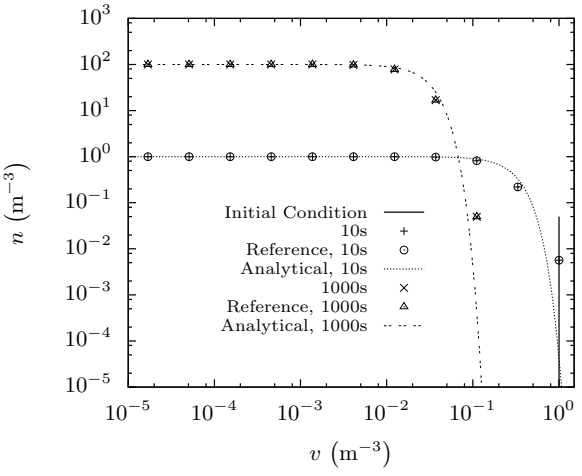

a) Number density, s=3

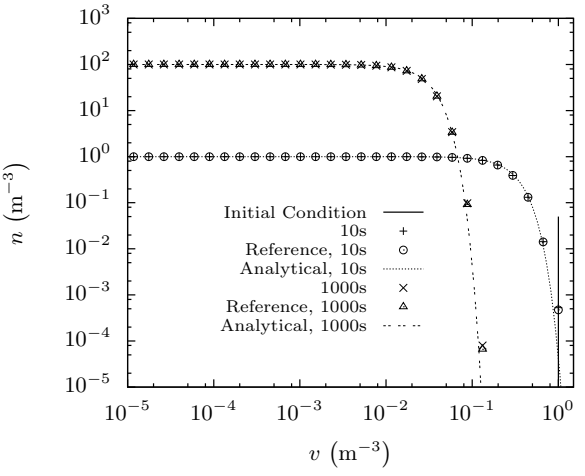

b) Number density, s=1.5

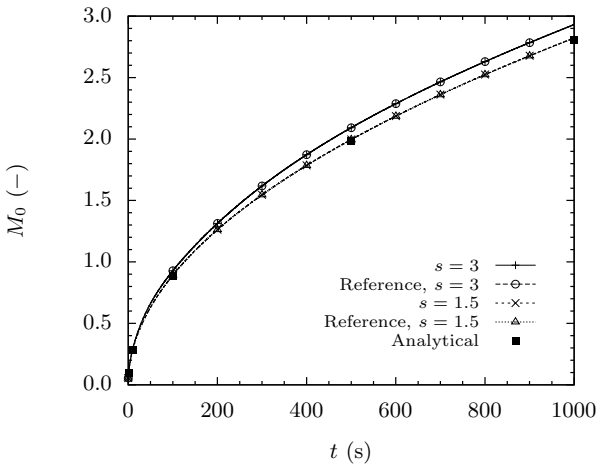

c) Number of particles

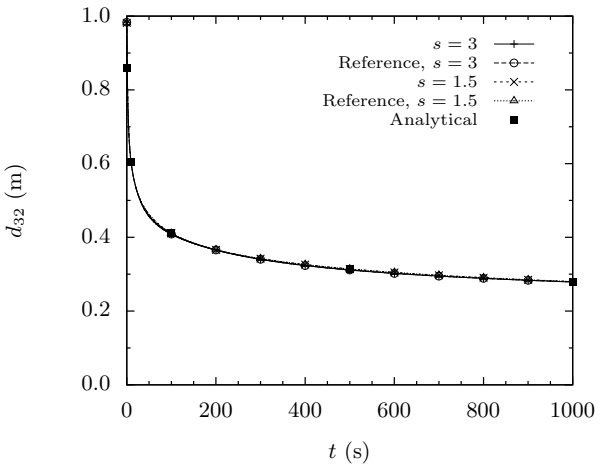

d) Sauter mean diameter

Figure 3: Results for Case 1

of the representative size x_1. It is obvious that the predictions for the power law kernel in combination with a uniform daughter size distribution are in good agreement with the analytical solution even for the coarse grid. However, a discretization error exits in both sets of numerical results for $s = 3$ in the large particle size range, where the initial number density gradient as well as the class width are large (see Fig. 3a). The transient variation of M_0 is shown in Fig. 3c. A slight over-prediction exists, if a coarse grid ($s = 3$) is applied. The discretization error vanishes as expected, if the resolution is increased by decreasing the value of s. The numerical and the analytical results are in a good agreement at $s = 1.5$ and the total particle number obtained by the new and the reference formulation are identical for both values of s. The Sauter mean diameter d_{32} is a key parameter for CFD simulations of particulate or bubbly flows, since it is used for many correlations for the interfacial transfer of momentum, heat and mass. Its transient variation is shown in Fig. 3d. In a pure breakage process, the mean size of particles decreases continuously. The effect of grid resolution is found to be negligible in this case. The predictions for both fine and coarse grids coincide with the analytical results and the reference solution.

Case 2. Unlike for the above uniform daughter size distribution, the probability of equal-sized breakage is the highest in the beta distribution given for this case. Figure 4a and 4b show a comparison between the predictions for the particle number density obtained by the reference and the new formulation. An analytical solution is not available for this case. It is found that the results deviate from each other toward the small particle size end for the coarse grid ($s = 3$), as shown in Fig. 4a. In addition, a grid-dependency of the results obtained by using the reference formulation is observed, while the new formulation behaves similar at both resolutions. The over-prediction of particle number on coarse grids by the reference formulation is discussed in Kumar & Ramkrishna (1996b) and Bayraktar (2014). With the refinement of the grid, the predictions of both formulations coincide with each other, see Fig. 4b. The corresponding predictions for the total number of particles as well as Sauter mean diameter for Case 2 are shown in Fig. 4c and Fig. 4d, respectively. Satisfying agreement is achieved for the Sauter mean diameter, which is mainly governed by the particles in the large size range. Nevertheless, the over-prediction of the total particle number by the Kumar & Ramkrishna (1996a) formulation at $s = 3$ due to the over-prediction of the birth rate of small particles is shown here as well.

Case 3. In case 3 the breakup model from the work of Coulaloglou & Tavlarides (1977) is adopted. In contrast to case 1 and 2, the breakup frequency is higher, which results in the effect that the majority of particles is concentrated at the smaller particle size end after a relatively short time period. The parameters used to determine the breakup rate are given at the beginning of Sect. 4. The number density function is plotted in Fig. 5a and 5b. The deviation between the two sets of results for the coarse grid is evident here as well. Yet they converge to one another for the finer grid. Figure 5c shows that in the first 30 s, the total particle number predicted by the reference and the new formulation are in quantitative agreement. With increasing time, however, the results diverge from each other for the coarse grid, and the new formulation predicts higher values than the reference formulation of Kumar & Ramkrishna (1996a). This deviation is caused by the treatment at the lower bound of the first class. Since v_1 is set to x_1, the birth rate of particles in the range $[0, x_1]$ due to

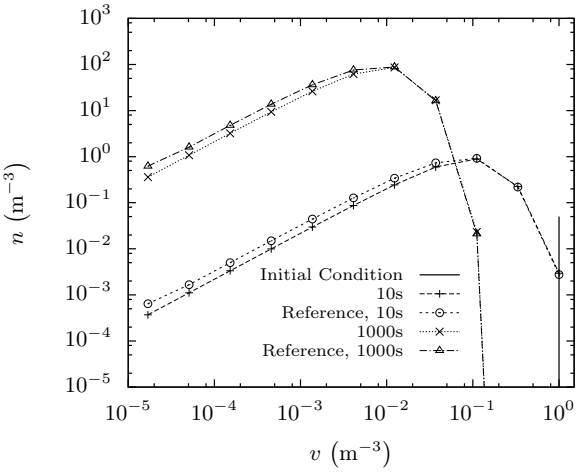

a) Number density, s=3

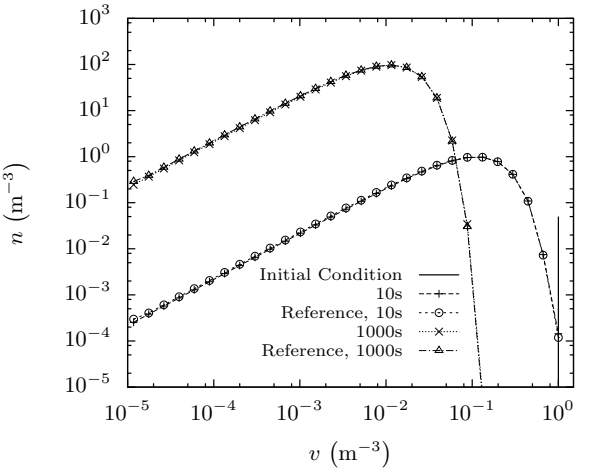

b) Number density, s=1.5

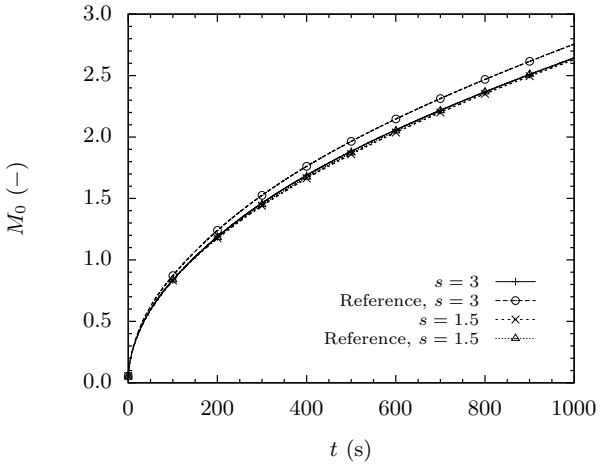

c) Number of particles

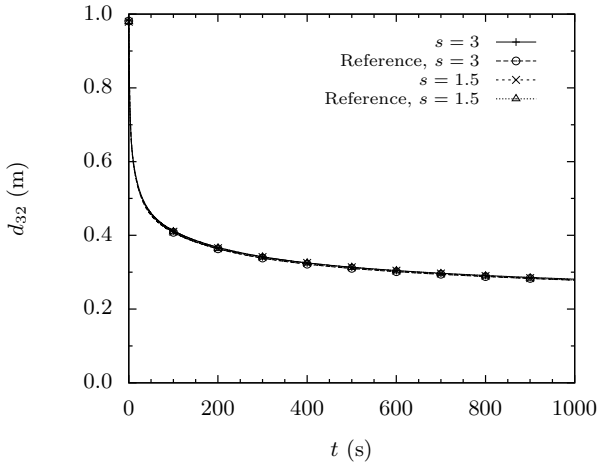

d) Sauter mean diameter

Figure 4: Results for Case 2

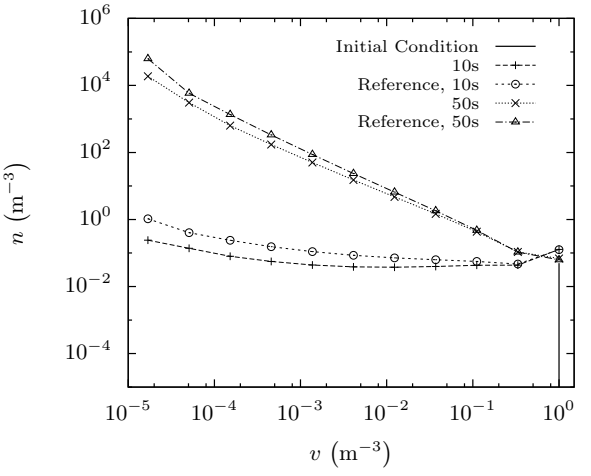

a) Number density, s=3

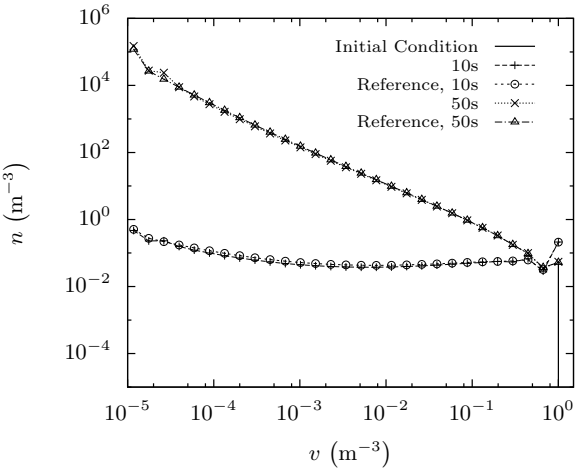

b) Number density, s=1.5

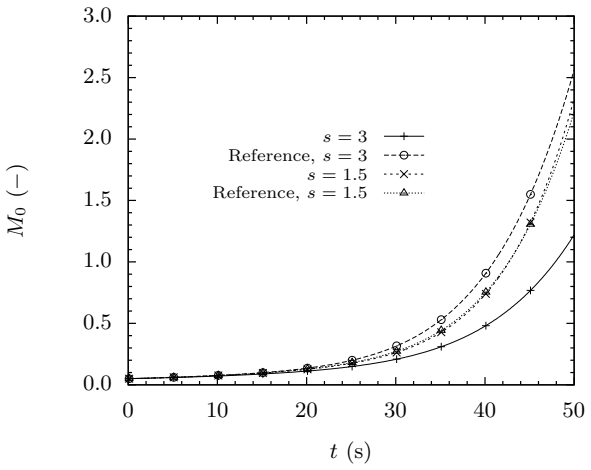

c) Number of particles

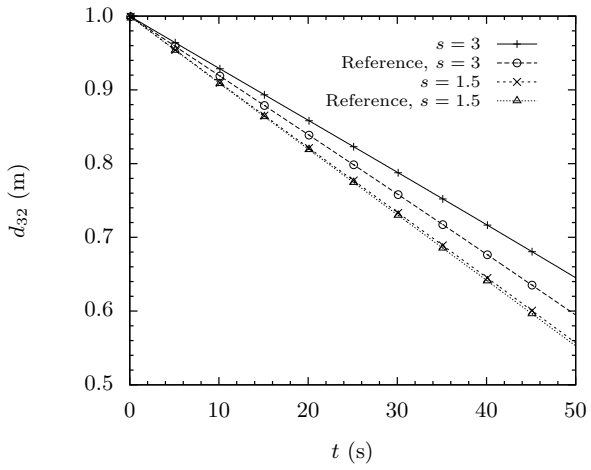

d) Sauter mean diameter

Figure 5: Results for Case 3

breakup of larger particles is not considered. The omitted parts,

$$\int_0^{x_1} N_j \Omega_t(x_j) \beta(v, x_j) \mathrm{d}v$$

for the reference formulation, and

$$N_j \Omega_t(x_j) \beta(x_1, x_j) \Delta v_1(j)$$

for the new one, are identical for constant β as in case 1 and of comparable magnitude for sufficiently large mother particle sizes x_j as in case 2. However, the difference becomes larger as the size of the breaking particles becomes smaller. The deviation depends on the features of the β function and the value of $\Delta v_0(j)$, and is responsible for the discrepancy between the methods. It should be mentioned though, that for a system with simultaneous coalescence and breakage, the discretization over the internal coordinate should ensure, that the number of particles in the first as well as the last size class remains zero. If this is the case, the above differences will be reduced. Furthermore, it is worth noting that limiting v_1 to x_1 is a necessity for the reference formulation, but not for the new formulation, which satisfies the overall balance between birth and death either way, provided that the death rate is calculated by Eq. 18. The temporal evolution of d_{32} is illustrated in Fig. 5d. In this case, the prediction by the new formulation also agrees well with the reference formulation if a sufficiently fine discretization is applied.

Case 4. The last case shows the behavior of the new and the reference formulation for partial breakup models like the model of Luo & Svendsen (1996). The predicted particle number density functions are shown in Fig. 6a and 6b, respectively. The two formulations deliver almost identical results for both grids. Figure 6c shows the evolution of total particle number. It is shown that the prediction using the new formulation almost coincides with the reference solution. According to the Luo & Svendsen (1996) model, the daughter size distribution should obey a U-shape function, which gives the highest probability for unequal-sized breakage. A steep gradient appears in the birth rate of daughter particles with sizes approaching zero or the mother particle size, respectively. Because of that, a large number of nodes is required for the numerical integration of Eq. 8 in these regions. Otherwise, the birth rate may be under-predicted. The temporal evolution of Sauter mean diameter in the first 50 s is depicted in Fig. 6d, with very similar predictions as well. In a word, comparable results are obtained with both formulations. However, the implementation of partial breakup models in the new formulation given by Eq. 17 and 18 is direct and efficient without any numerical integrations.

5. Conclusions

A discrete formulation of the PBE for binary breakage is presented. It is shown to be applicable for both frameworks of breakup modeling, i.e., total and partial breakup kernels with a separate or incorporated function for the daughter size distribution. Its validity is tested for various cases with different breakup models and daughter size distributions, using an analytical solution as well as reference solutions based on the work of Kumar & Ramkrishna (1996a). Two geometric grids are applied and the results for particle number density, total number and Sauter mean diameter predicted by the new and the reference formulation coincide for the finer

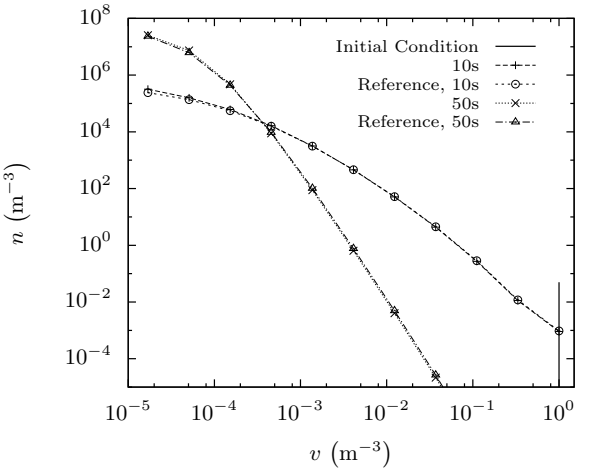

a) Number density, s=3

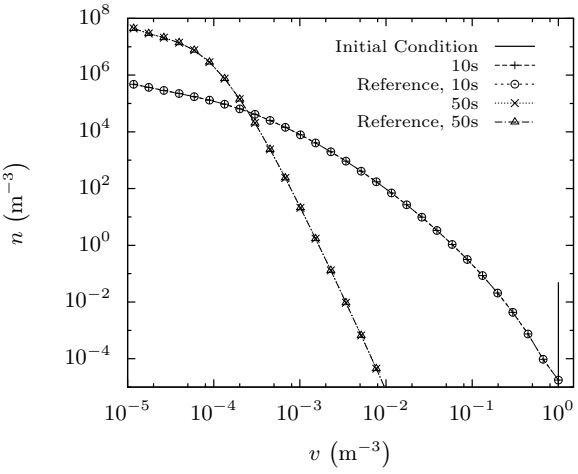

b) Number density, s=1.5

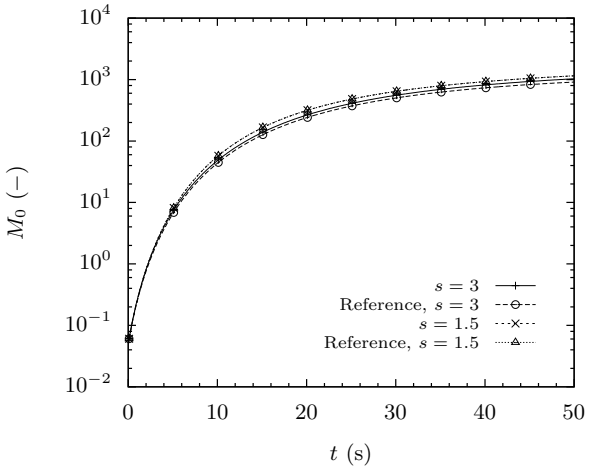

c) Number of particles

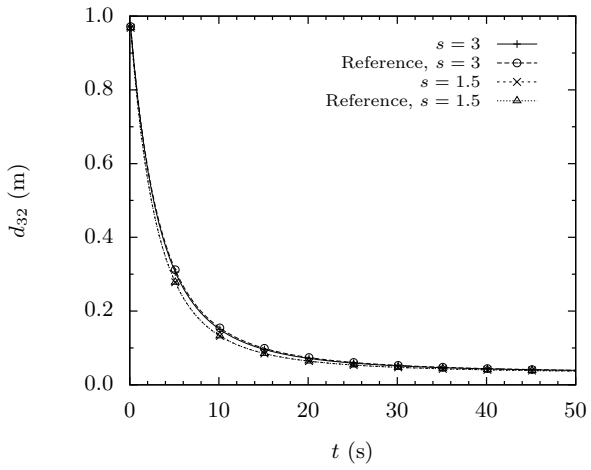

d) Sauter mean diameter

Figure 6: Results for Case 4

grid. Both formulations ensure the preservation of numbers and mass. The preservation of other moments may be achieved by adapting the weight function Y_{ijk} (Eq. 14) accordingly, as presented by Kumar & Ramkrishna (1996a). Furthermore, the formulation is flexible on the discritization and applicable for a constant or increasing class width, i.e., uniform and geometric grids with section spacing factors $s \geq 1$. The advantage of the new formulation is the possibility to directly implement partial breakup models (Luo & Svendsen, 1996; Liao et al., 2015), which provide the breakup rate between a mother and a daughter particle directly. It avoids the extraction of the daughter size distribution by means of numerical integration, which introduces considerable numerical cost and is required for the reference formulation, making it more suitable for the coupling with CFD.

Nomenclature

B	birth rate	$\mathrm{m}^{-3}\,\mathrm{m}^{-3}\,\mathrm{s}^{-1}$
D	death rate	$\mathrm{m}^{-3}\,\mathrm{m}^{-3}\,\mathrm{s}^{-1}$
d	bubble diameter	m
M	moment of number density distribution	m^{-3}
n	number density	$\mathrm{m}^{-3}\,\mathrm{m}^{-3}$
N	number concentration	m^{-3}
s	section spacing factor	$-$
v, x	particle volume, representative volume	m^{-3}

Greek letters

α	void fraction of particles	$-$
β	size distribution probability of daughter particles	m^{-3}
Δv	class width	m^{-3}
δ	Dirac delta function	$-$
ϵ	turbulent dissipation rate	$\mathrm{m}^2\,\mathrm{s}^{-3}$
η	Kolmogorov length scale	m
μ	liquid dynamic viscosity	$\mathrm{Pa\,s}$
ρ	density	$\mathrm{kg\,m}^{-3}$
σ	surface tension coefficient	$\mathrm{N\,m}$
Ω_p	partial breakup rate	$\mathrm{s}^{-1}\,\mathrm{m}^{-3}$
Ω_t	total breakup rate	s^{-1}

Subscripts

g	gas
i, j, k	indexes of size classes
l	liquid
p	partial
t	total
0	zeroth moment

References

Bannari, R., Kerdouss, F., Selma, B., Bannari, A., & Proulx, P. (2008). Three-dimensional mathematical modeling of dispersed two-phase flow using class method of population balance in bubble columns. *Computers & Chemical Engineering*, *32*, 3224–3237.

Batterham, R. J., Hall, J. S., & Barton, G. W. (1981). Pelletizing kinetics and simulation of full scale balling circuits. In *3rd International Symposium on Agglomeration* (pp. A136–A150).

Bayraktar, E. (2014). *Numerical aspects of population balance equations coupled to computational fluid dynamics*. Ph.D. thesis Technical University of Dortmund Dortmund, Germany.

Bellot, J.-P., De Felice, V., Dussoubs, B., Jardy, A., & Hans, S. (2014). Coupling of CFD and PBE calculations to simulate the behavior of an inclusion population in a gas-stirring ladle. *Metallurgical and Materials Transactions B*, *45*, 13–21. http://dx.doi.org/10.1007/s11663-013-9940-7.

Bove, S. (2005). *Computational fluid dynamics of gas-liquid flows including bubble population balances: Ph.D. thesis*. Ph.D. thesis Aalborg University Esbjerg Esbjerg, Denmark.

Chen, P., Dudukovic, M. P., & Sanyal, J. (2005). Three-dimensional simulation of bubble column flows with bubble coalescence and breakup. *AIChE Journal*, *51*, 696–712.

Cheung, S. C. P., Deju, L., Yeoh, G. H., & Tu, J. Y. (2013). Modeling of bubble size distribution in isothermal gas-liquid flows: Numerical assessment of population balance approaches. *Nuclear Engineering and Design*, *265*, 120–136.

Coulaloglou, C. A., & Tavlarides, L. L. (1977). Description of interaction processes in agitated liquid-liquid dispersions. *Chemical Engineering Science*, *32*. https://doi.org/10.1016/0009-2509(77)85023-9.

Engquist, B., Tornberg, A.-K., & Tsai, R. (2005). Discretization of dirac delta functions in level set methods. *Journal of Computational Physics*, *207*, 28–51. https://doi.org/10.1016/j.jcp.2004.09.018.

Gelbard, F., & Tambour, Y. S. (1980). Sectional representations for simulating aerosol dynamics. *Journal of Colloid and Interface Science*, *76*, 541–556. https://doi.org/10.1016/0021-9797(80)90394-X.

Goodson, M., & Kraft, M. (2004). Simulation of coalescence and breakage: An assessment of two stochastic methods suitable for simulating liquid-liquid extraction. *Chemical Engineering Science*, *59*, 3865–3881. https://doi.org/10.1016/j.ces.2004.05.029.

Hagesaether, L., Jakobsen, H. A., & Svendsen, H. F. (2002). A model for turbulent binary breakup of dispersed fluid particles. *Chemical Engineering Science*, *57*, 3251–3267. https://doi.org/10.1016/S0009-2509(02)00197-5.

Hill, D., Wang, D., Gosman, A., & Issa, R. (1995). Numerical prediction of two-phase bubbly flow in a pipe. In *Proc. 2rd Int. Conf. on Multiphase Flow. Kyoto* (pp. MO3–1–MO3–6).

Hounslow, M. J., Ryall, R. L., & Marshall, V. R. (1988). A discretized population balance for nucleation, growth, and aggregation. *AIChE Journal*, *34*, 1821–1832.

Hulburt, H. M., & Katz, S. (1964). Some problems in particle technology: A statistical mechanical formulation. *Chemical Engineering Science*, *19*, 555.

Jakobsen, H. A. (2008). *Chemical Reactor Modeling: Multiphase Reactive Flows*. (1st ed.). Heidelberg, Germany: Springer-Verlag Berlin Heidelberg. https://doi.org/10.1007/978-3-540-68622-4.

Kruis, F. E., Wei, J., van der Zwaag, T., & Haep, S. (2012). Computational fluid dynamics based stochastic aerosol modeling: Combination of a cell-based weighted random walk method and a constant-number monte-carlo method for aerosol dynamics. *Chemical Engineering Science*, *70*, 109–120. https://doi.org/10.1016/j.ces.2011.10.040.

Kumar, S., & Ramkrishna, D. (1996a). On the solution of population balance equations by discretization-I. a fixed pivot technique. *Chemical Engineering Science*, *51*, 1311–1342.

Kumar, S., & Ramkrishna, D. (1996b). On the solution of population balance equations by discretization-II. a moving pivot technique. *Chemical Engineering Science*, *51*, 1333–1342.

Laakkonen, M., Alopaeus, V., & Aittamaa, J. (2006). Validation of bubble breakage, coalescence and mass transfer models for gas-liquid dispersion in agitated vessel. *Chemical Engineering Science*, *61*, 218–228.

Lee, C.-H., Erickson, L. E., & Glasgow, L. A. (1987). Dynamics of bubble size distribution in turbulent gas-liquid dispersions. *Chemical Engineering Communications*, *61*, 181–195. https://doi.org/10.1080/00986448708912038.

Lehr, F., Millies, M., & Mewes, D. (2002). Bubble-size distributions and flow fields in bubble-columns. *AIChE Journal*, *48*, 2426.

Li, Z., Kessel, J., Grünewald, G., & Kind, M. (2013). Coupled CFD-PBE simulation of nucleation in fluidized bed spray granulation. *Drying Technology*, *31*, 1888–1896. https://doi.org/10.1080/07373937.2013.840649.

Liao, Y., Lucas, D., Krepper, E., & Schmidtke, M. (2011). Development of a generalized coalescence and breakup closure for the inhomogeneous MUSIG model. *Nuclear Engineering and Design*, *241*, 1024–1033.

Liao, Y., Rzehak, R., Lucas, D., & Krepper, E. (2015). Baseline closure model for dispersed bubbly flow: Bubble-coalescence and breakup. *Chemical Engineering Science*, *122*, 336–349. https://doi.org/10.1016/j.ces.2014.09.042.

Luo, H., & Svendsen, H. F. (1996). Theoretical model for drop and bubble-breakup in turbulent dispersions. *AIChE Journal*, *42*, 1225–1233.

Madadi-Kandjani, E., & A., P. (2015). An extended quadrature-based moment method with log-normal kernel density functions. *Chemical Engineering Science*, *131*, 323–339.

Marchal, P. (1988). Crystallization and precipitation engineering-I. an efficient method for solving population balance in crystallization with agglomeration. *Chemical Engineering Science*, *43*, 59–67.

Martinez-Bazan, C., Montanes, J. L., & Lasheras, J. C. (1999). On the breakup of an air bubble injected into a fully developed turbulent flow. part 1. breakup frequency. *J. Fluid Mech*, *401*, 157–182.

McCoy, B. J., & Madras, G. (2003). Analytical solution for a population balance equation with aggregation and fragmentation. *Chemical Engineering Science*, *58*, 3049–3051. https://doi.org/10.1016/S0009-2509(03)00159-3.

Meimaroglou, D., & Kiparissides, C. (2007). Monte carlo simulation for the solution of the bi-variate dynamic population balance equation in batch particulate systems. *Chemical Engineering Science*, *62*, 5295–5299. https://doi.org/10.1016/j.ces.2006.11.032.

Metzger, L. (2016). The influence of mixing on fast precipitation processes – a coupled 3d cfd-pbe approach using the direct quadrature method of moments (dqmom). *Chemical Engineering Science*, .

Pinar, Z. (2015). Analytical solution of population balance equation involving growth, nucleation and aggregation in terms of auxiliary equation method. *Applied Mathematics & Information Sciences*, *9*, 2467–2475.

Ramkrishna, D. (1985). The status of population balances. *Rev. Chem. Eng.*, *3*, 49–95.

Ramkrishna, D. (2000). *Population balances: Theory and applications to particulate systems in engineering*. Academic Press Inc.

Ramkrishna, D., & Singh, M. R. (2014). Population balance modeling: current status and future prospects. *Annual Review of Chemical and Biomolecular Engineering*, *5*, 123–146. https://doi.org/10.1146/annurev-chembioeng-060713-040241.

Randolph, A. D. (1964). A population balance for countable entities. *The Canadian Journal of Chemical Engineering*, *42*, 280–281. https://doi.org/10.1002/cjce.5450420612.

Sen, M., Barrasso, D., Singh, R., & Ramachandran, R. (2014). A multi-scale hybrid cfd-dem-pbm description of a fluid-bed granulation process. *Processes*, *2*, 89–111. https://doi.org/10.3390/pr2010089.

Singh, R. (2014). Adomian decomposition method for solving fragmentation and aggregation population balance equations. *Journal of Applied Mathematics and Computing*, (pp. 1–31). https://doi.org/10.1007/s12190-014-0802-5.

Thomas, R. J. (2013). Particle size and pathogenicity in the respiratory tract. *Virulence*, *4*, 847–858. https://doi.org/10.4161/viru.27172.

Tsouris, C., & Tavlarides, L. L. (1994). Breakage and coalescence models for drops in turbulent dispersions. *AIChE Journal*, *40*, 395–406. https://doi.org/10.1002/aic.690400303.

Vanni, M. (1999). Discretization procedure for the breakage equation. *AIChE Journal*, *45*, 916–919. https://doi.org/10.1002/aic.690450422.

Vanni, M. (2000). Approximate population balance equations for aggregation–breakage processes. *Journal of Colloid and Interface Science*, *221*, 143–160. https://doi.org/10.1006/jcis.1999.6571.

Wang, T., & Wang, J. (2007). Numerical simulations of gas-liquid mass transfer in bubble columns with a cfd-pbm coupled model. *Chemical Engineering Science*, *62*, 7107–7118.

Wang, T., Wang, J., & Jin, Y. (2003). A novel theoretical breakup kernel function for bubbles/droplets in a turbulent flow. *Chemical Engineering Science*, *58*, 4629–4637. https://doi.org/10.1016/j.ces.2003.07.009.

Wick, A., Nguyen, T.-T., Laurent, F., Fox, R. O., & Pitsch, H. (2017). Modeling soot oxidation with the extended quadrature method of moments. *Proceedings of the Combustion Institute*, *36*, 789–797. https://doi.org/10.1016/j.proci.2016.08.004.

Xing, C., Wang, T., Guo, K., & Wang, J. (2015). A unified theoretical model for breakup of bubbles and droplets in turbulent flows. *AIChE Journal*, *61*, 1391–1403. https://doi.org/10.1002/aic.14709.

Yuan, C., Laurent, F., & Fox, R. O. (2012). An extended quadrature method of moments for population balance equations. *Journal of Aerosol Science*, *51*, 1–23. https://doi.org/10.1016/j.jaerosci.2012.04.003.

Zhao, H., & Ge, W. (2007). A theoretical bubble breakup model for slurry beds or three-phase fluidized beds under high pressure. *Chemical Engineering Science*, *62*, 109–115. https://doi.org/10.1016/j.ces.2006.08.008.

Ziff, R. M., & McGrady, E. D. (1985). The kinetics of cluster fragmentation and depolymerisation. *Journal of Physics A: Mathematical and General*, *18*, 3027.